

PAPER • OPEN ACCESS

## A comparison of lineament and fracture trace extraction from LANDSAT ETM+ panchromatic band and panchromatic aerial photograph in Gunungsewu karst area, Java-Indonesia

To cite this article: E Haryono *et al* 2016 *IOP Conf. Ser.: Earth Environ. Sci.* **47** 012026

View the [article online](#) for updates and enhancements.

### Related content

- [Structure-geochemical zoning of Topoininsk gold-ore field \(Gorny Altai\)](#)  
T V Timkin, D S Lavrov, O Y Askanakova et al.
- [Study for urbanization corresponding to socio-economic activities in Savannaket, Laos using satellite remote sensing](#)  
S Kimijama and M Nagai
- [Identification, evaluation and change detection of highly sensitive wetlands in South-Eastern Sri Lanka using ALOS \(AVNIR2, PALSAR\) and Landsat ETM+ data](#)  
Ajith Gunawardena, Tamasha Fernando, Wataru Takeuchi et al.

# A comparison of lineament and fracture trace extraction from LANDSAT ETM+ panchromatic band and panchromatic aerial photograph in Gunungsewu karst area, Java-Indonesia

E Haryono<sup>1</sup>, B S Widartono<sup>1</sup>, H Lukito<sup>2</sup>, and S B Kusumayuda<sup>2</sup>

<sup>1</sup>Faculty of Geography, The University of Gadjah Mada, Yogyakarta, Indonesia

<sup>2</sup>Faculty of Mineral Technology, UPN Veteran University, Yogyakarta, Indonesia

Email: e.haryono@geo.ugm.ac.id

**Abstract.** This paper aims at exploring interpretability of the panchromatic band of Landsat Enhanced Thematic Mapper Plus (ETM+) compared to the panchromatic aerial photograph in lineament and fracture trace extraction. Special interest is addressed to karst terrain where lineaments and fracture traces are expressed by aligned valleys and closed depressions. The study area is a single aerial photographic coverage in the Gunungsewu Karst, Java-Indonesia which is characterized by a lineament-controlled cone karst and labyrinth-cone karst. The result shows that the recording time of the Landsat ETM+ with respect to the shadow resulting from the sun illumination angle is the key factor in the performance of lineament and fracture traces extraction. Directional filtering and slicing techniques significantly enhance the lineament interpretability of the panchromatic band of Landsat ETM+. The two methods result in more lineaments and fracture traces which T-test affirm in 0.001 and 0.004 significant levels. Length based lineament analysis attains a better result compared to frequency based analysis.

## 1. Introduction

Application of remote sensing on lineament mapping has been the subject of study since the early development of remote sensing techniques. Lineament owes its importance from the fact that lineaments are associated with structural. These are mostly the trace of discontinuities, such as bedding planes, faults, joints fractures with the ground surface [33]. O'Leary *et al.*, [16] defined a lineament as a simple or composite linear feature of surface whose parts are aligned in a rectilinear or slightly curvilinear relationship and which differ from the pattern of adjacent features and presumably reflects some sub-surface phenomenon. Parizek [18], considered a lineament is a 1.5 km length or more linear feature and a fracture trace is a linear features which is less than 1.5 km long.

Remote sensing techniques have more interest in lineament mapping due to their ability to provide more factual earth surface information, as compared to those of topographical maps. Lineament and fracture traces are readily interpreted and analyzed through pattern recognition in today broad coverage of remote sensing images. Moreover, satellite images with the availability of multispectral information and image enhancement techniques provide the opportunity to analyze relatively more



reliable lineament and fracture traces. The wide ground coverage and better resolution of satellite images also enable regional as well as local lineament analysis [1, 14, 15, 19, 29, 30, 32]. Therefore interpretation of lineament and fracture traces from remote sensing images is much easier than that from topographical maps or even from field investigation.

Field investigation prepared by conventional field mapping techniques cannot identify the entire extent of lineaments existing in an area. On the contrary, remote sensing images enable to detect large lineaments which extend far beyond the field surveyor observation. The potential application related to lineament and fracture traces are mostly for groundwater exploration [4, 5, 13, 24].

Analyzing lineaments and fracture traces in karst regions has also been an interesting subject of study. The use of remote sensing in lineament analysis of karst areas provides meaningful information since karstification is often controlled by preexisting structures, such as joints, fractures, and faults. Those structures often control the doline or dry valley development leading to an alignment of dolines or dry valleys [2, 7, 13]. Lineaments and fracture traces are associated with underground river passages [4, 8, 9, 13, 18]. Lineaments and fracture traces have also meaningful information for cave development [10].

Lineament and fracture traces identification from remote sensing data can be achieved either using manual [2, 4, 7] or automated techniques [1, 15, 19, 31]. These two techniques have their own advantages and disadvantages. Lineament and fracture trace interpretation from aerial photograph or non-enhanced satellite images produce inconsistent results. Variations in lineament patterns can occur between interpretations of the same scene by one observer on multiple occasions as well as between interpretations of the scene by several observers. There is also the problem of assessing the similarity or the differences between interpretations from two different scenes having similar geological patterns [11]. Automated interpretation on the other hand provides more objective lineament features but is not able to differentiate geological lineaments from non-geological lineaments such as roads, land use borders or electricity lines.

This paper is aimed at exploring lineament interpretability of the panchromatic band of Landsat Enhanced Thematic Mapper Plus (ETM+) compared to the panchromatic aerial photographs. Geologically, the study area is dominated by Miocene coral limestone of Wonosari Formation (Figure 1). The study area is a single aerial photographic coverage in the Gunungsewu Karst, Java-Indonesia which is characterized by a lineament-controlled cone karst and labyrinth-cone karst (Figure 2). The Wonosari Formation was uplifted during the late Pliocene and/or early Pleistocene and dips gently southwards at about 2° gradient. Dominant land covers of the area are dry fields and bare lands. Dry fields occupy the bottom of aligned dry valleys whereas bare lands with scattered perennial crops dominate the karst hill land covers. No land cover/land use changes have been reported taking place for the last four decades.

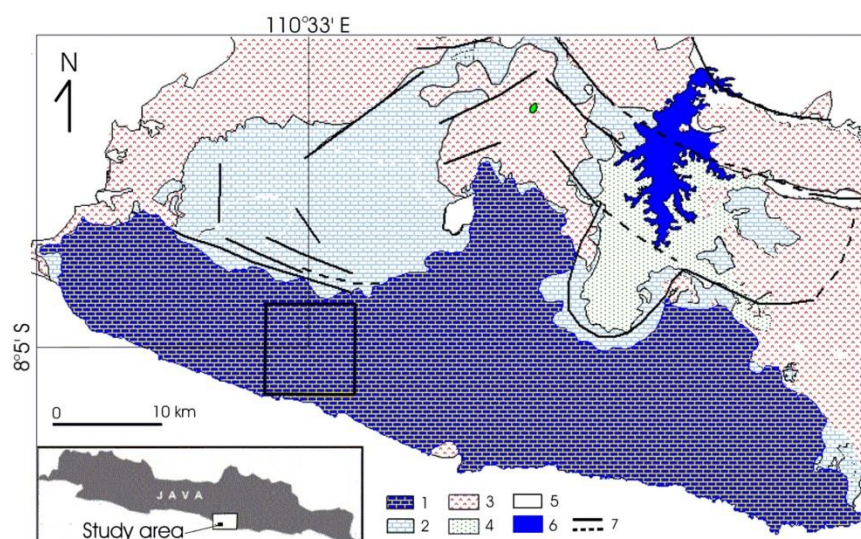


**Figure 1.** The study area and its geological setting : 1) Gunungsewu Karst 2) Non-karstified carbonate rocks 3) Tertiary volcanic clastic rocks, 4) Pleistocene alluvium, 5) Quaternary pyroclastics and alluvium, 6) Reservoir, 7) Fault and flexures [Compiled from 21, 32]



**Figure 2.** Photograph depicting part of Gunungsewu Karst which is characterized by conical hills and aligned dry valleys

## 2. Materials and Methods

The images used in this paper are panchromatic aerial photographs (1:50 000, September 1993) and Landsat ETM+ (row 066 path 119, June 2000). The image processing in the present paper was conducted using ILWIS Version 3.1, whereas lineament and statistical analysis were conducted using Rockworks99 and SPSS 10 respectively. Before being processed, the aerial photograph was scanned in 200 dpi resolution. Such resolution is quite reasonable in this research since the original aerial photograph is 1:50,000 scale and the scanned image was interpreted on-screen at 1:25,000 scale. The scanned version was then geometrically corrected with polynomial methods. Seven Ground Control Points (GCPs) were taken in geometric correction resulting in 4.475 RMS errors. The geometric correction was also applied over the Landsat ETM+ raw images with 5 control points resulting in RMS error of 0.591. The selected Landsat ETM+ panchromatic band (band 8) was then stretched using histogram equalization techniques.

Two procedures were employed during interpretation. Firstly, interpretation was conducted by a group of 16 fourth year students from the Physical Geography Department. The students were divided into two groups where the first group interpreted the aerial photograph and the second one was asked to interpret the panchromatic band of Landsat ETM+. Time allocation for interpretation was 15 minutes. This procedure is intended to get a first impression of the aerial photograph and the original panchromatic band of Landsat ETM+ performances in depicting lineaments and fracture traces. Lineament interpretation was carried out on the printed aerial photograph and Landsat image on which the geometric correction and histogram equalization stretch technique have been applied. The printer used in this research is a 1200 dpi resolution printer. Both images were printed in the scale of 1: 50 000.

Secondly, interpretation was conducted by the first author through on screen digitizing over scanned aerial photographs and the pre-enhanced panchromatic band of Landsat ETM+. In this procedure the panchromatic band of Landsat ETM+ was first filtered to enhance the lineament features by applying Sobel kernels convolution in four principal directions (Table 1). These four spatial domain filters have been found very helpful in enhancing lineament features [29]. The filtered images were then visualized in black and white presentation through slicing procedure in order to depict extreme contrast visualization between shaded aligned valleys and illuminated aligned karst hills.

**Table 1.** Sobel kernel in four principle directions

N-S			NE-SW			E-W			NW-SE		
-1	0	1	-2	-1	0	-1	-2	-1	0	1	2
-2	0	2	-1	0	1	0	0	0	-1	0	1
-1	0	1	0	1	2	1	2	1	-2	-1	0

In order to get more objective and consistent interpretation the author took into account some rules as follows:

- the images being interpreted were zoomed in to 1 : 25 000 scale,
- lineament delineation in the aerial photograph was performed along the bottom of an aligned valley (see Figure 3a),
- the features considered as lineaments in the sliced-filtered images are continuous aligned black pixels without any interrupted white pixels (see Figure 3b),
- lineaments which were less than 100 meters long were not included.

To avoid redundant lineaments, on screen interpretation of the four sliced-filtered images was performed consecutively by putting the image as background one by one starting from Sobel-NWSE and continued by Sobel-NS, Sobel-EW, and Sobel-SENW. If lineaments had been delineated from a certain filtered image, the same lineaments were not delineated again from the other filtered images where delineation only focuses on additional lineaments which were not depicted in the previously interpreted image. Thus, the lineament map derived from four filtered images was overlaid into a single lineament map.

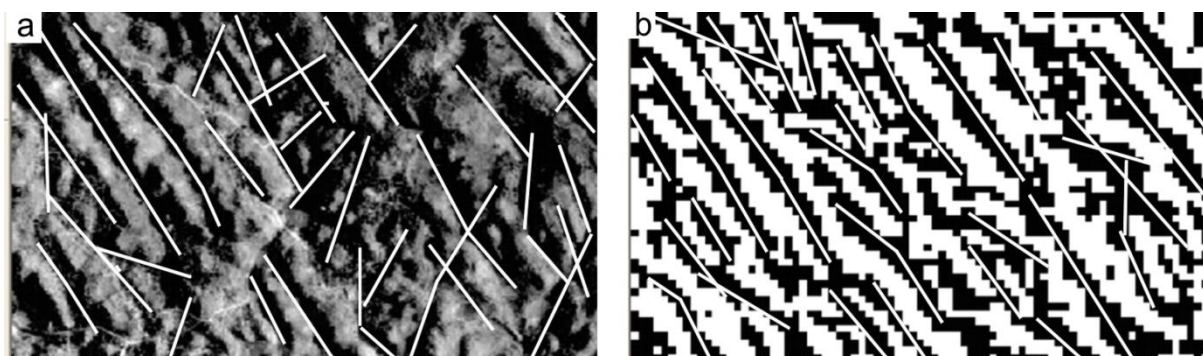


**Figure 3.** Examples of lineament delineation from panchromatic aerial photograph and slice-filtered image

### 3. Results and Discussion

#### 3.1. Result

Sample areas derived from the image processing are presented in Figure 4. With a quick look at the images, it is immediately clear that the panchromatic aerial photograph depicts better features of lineaments and fracture traces compared to the band-8 of Landsat ETM+ (Figure 4a and 4b). Less detailed morphological features are the reason for less distinct lineaments in the stretched band 8 image compared to the aerial photograph. This is quite reasonable since the band 8 of Landsat ETM+ has coarser resolution. The less striking shadow must also be accounted for the explanation of the less distinctive lineament features of the band 8 in the Landsat ETM+. Observing Figure 4, the lineaments in the SW-NE azimuth depicted in the band 8 are not as clear as that in the aerial photograph.

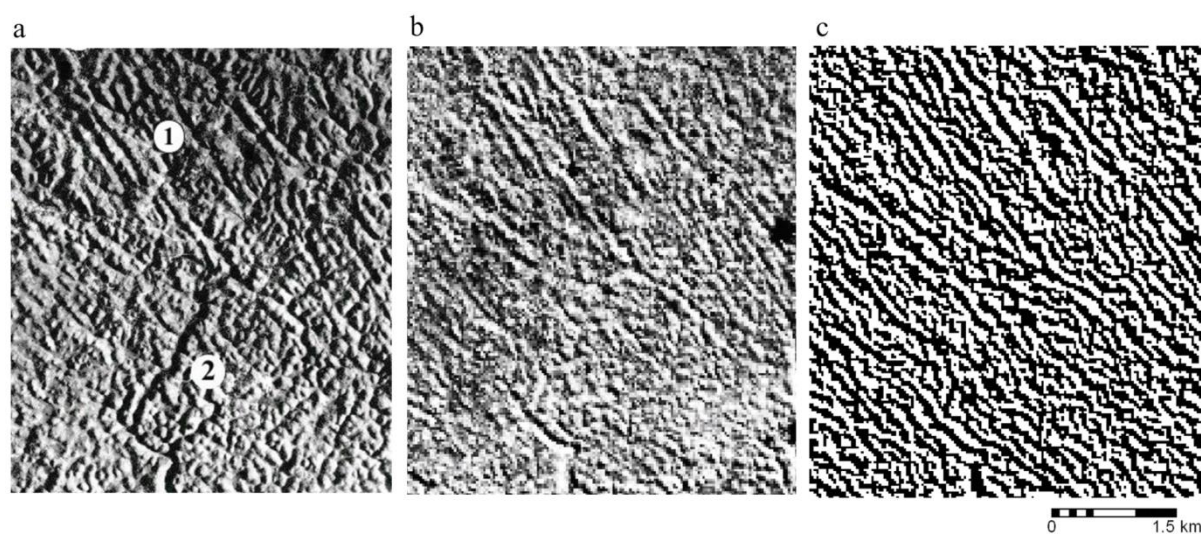


**Figure 4.** Lineaments depicted in (a) panchromatic aerial photograph, (b) panchromatic band of Landsat ETM+ and (c). Sliced-filtered band 8. Lineaments with SE-NW azimuth are presented clearly in both images (around no 1). Whereas, lineaments with NE-SW azimuth are not depicted well in the panchromatic band of Landsat ETM+. However they are still easily recognized in the aerial photograph (left of symbol 2 in 3a).

A better expression of lineaments and fracture traces in the panchromatic aerial photograph compared to the Landsat ETM+ band 8 is also confirmed by lineaments found by the students (Table 2). The group of seven students who were responsible for the aerial photograph interpretation produced more lineaments both in terms of the number and the length of lineaments and fracture traces. One tail T-test analysis indeed confirms the better result of aerial photographic interpretation in 0.002 significant level. However, the two groups have the same results with respect to dominant lineament azimuth. Variability in the delineation between the two groups as represented by the standard deviation does not indicate much difference. Such figures reveal that inconsistency among individuals is encountered during lineament delineation, in agreement with the findings suggested by Hutington and Raiche [11]. However, deviation in this paper is quite reasonable since the students were provided only approximately 15 minutes to do the interpretation. This short time is provided to make sure that results of interpretation are only derived from their first expression about the lineaments and fracture traces depicted in the images. Additional time and more experienced interpreters will obviously cause less variability.

**Table 2.** Lineament and fracture trace summary statistics acquired from the panchromatic aerial photograph and the band 8 of Landsat ETM+ (conducted by 16 students)

Type of Image	Numb interpreter)	Number of Lineaments		Length of Lineaments		Dominant Azimuth
		Average	Standard Deviation	Average (m)	Standard deviation	
Panchromatic Aerial Photograph	7	169.4	34	113 203.02	34 583.88	320-330
Band 8 of Landsat ETM+	9	132.6	49.2	98 084.04	21 338.46	320-330

Filtering and slicing techniques, however, result in better lineament and fracture trace appearance of Landsat ETM+ band 8 (Figure 4c). Contrast feature of binary presentation have made possible the lineaments and fracture traces be identified easier compared to that in the original Landsat ETM+ band 8 image as well as in the aerial photograph. This result confirms the previous work by Haryono

*et al.*, [9] and Kresic [13], suggesting that slicing is successful in enhancing lineaments of karst terrain. Further and more careful interpretation conducted by the author over the slice-filtered band 8, nevertheless confirmed the above mention finding. Directional filtering and slicing enhancement techniques do increase significantly lineament interpretability of the Landsat ETM+ band 8 image. On screen presentation make the lineaments and fracture traces more obvious. Software facility of on screen zooming is very helpful especially within areas with dense lineaments.

Table 3 and Figure 5 show that more lineaments and fracture traces are extracted from the slice-filtered band 8 than from the panchromatic aerial photograph. This result is also affirmed by T-test statistical analysis upon the lineament length in one-tile significant level of 0.004. This paper shows that the slice-filtered band 8 is very helpful in the karst area where topographic expression of lineaments is not obvious, such as in the upright corner of the area (Figure 5). Another explanation which is accounted for the straightforward delineation from the sliced-filtered image is the contrast expression between aligned valleys (shade areas) and the opposite positive relief.

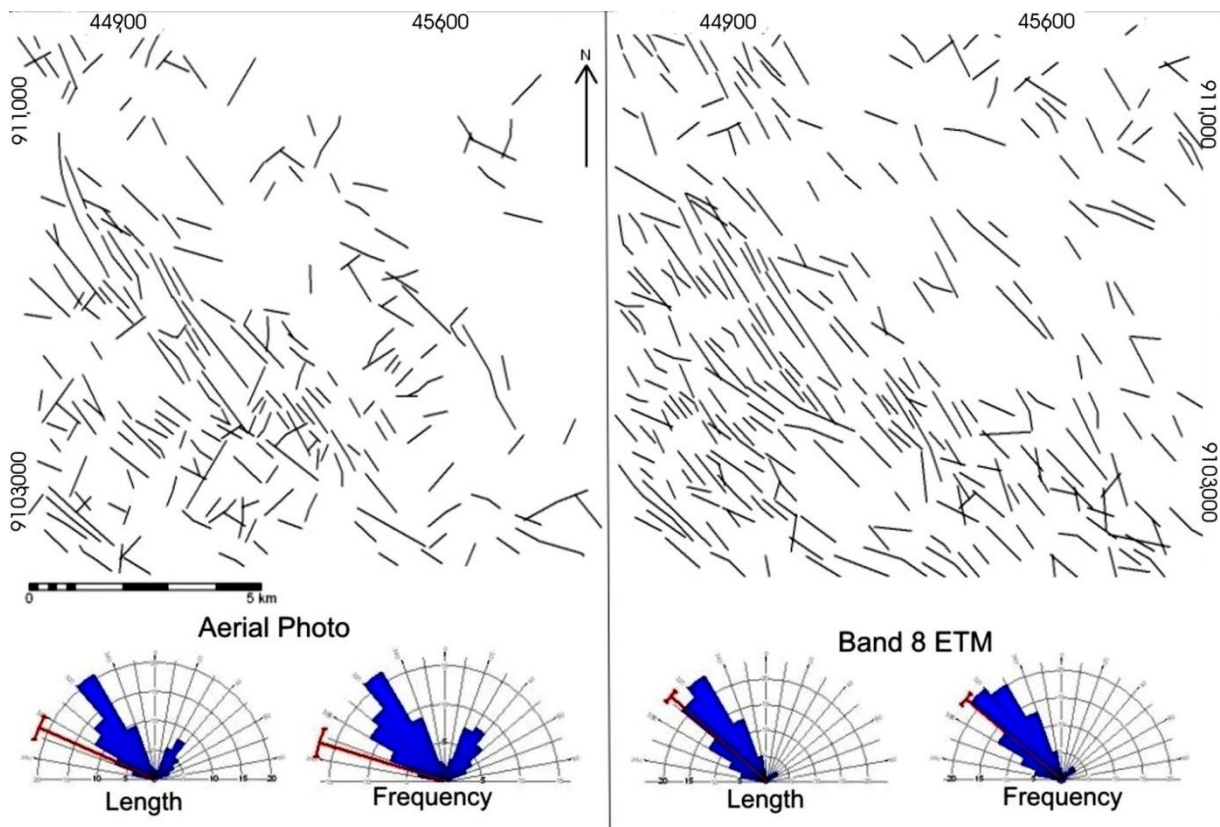


**Figure 5.** Lineaments and rose diagrams extracted from the panchromatic aerial photograph and Landsat ETM+ band 8 after being subjected to slicing and directional filtering

**Table 3.** Lineament and fracture trace summary statistics acquired from the panchromatic aerial photograph and the slice-filtered band 8 of Landsat ETM+ (conducted by the first author). Percentage in brackets

Type of Image	By Length (m)	Vector Statistics				Mean	Dominant vector
		NS	NE-SW	EW	NW-SE		
Panchromatic Aerial Photograph	163 757.2 (100)	17 857.1 (10.9)	35 921.8 (21.9)	11 985.1 (7.3)	97 993.3 (59.8)	294	320-330

Band 8 of Landsat ETM+	232 075.6 (100)	20 196.8 (8.7)	16 430.4 (7.1)	22 484.1 (9.7)	174 122.6 (75)	131.7	320-330
	<b>By Number</b>						
Panchromatic Aerial Photograph	276 (100)	37 (13.4)	69 (25)	22 (7.9)	148 (53.6)	287	320-330
Band 8 of Landsat ETM+	346 (100)	32 (9.2)	30 (8.7)	32 (9.2)	252 (72.8)	310	310-320

Scrutiny over vector distribution, lineaments and fracture traces derived from aerial photograph and the slice-filtered image unveils a slightly different result which can be observed from the rose diagrams and from Table 3. The difference which is readily observed is higher frequency of the NE-SW vector in the aerial photograph than that in the slice-filtered band 8. Such result does not necessarily indicate that enhancing Landsat ETM+ band 8 through filtering and enhancing techniques is worse compared to the aerial photograph. The reason for this must be attributed to less shadows in the NE-SW direction in band 8 of Landsat ETM+. As mentioned previously, the original Landsat ETM+ band has intrinsically little shadow in the NE-SW direction. Hence Sobel directional filter applied in the present paper does not help much. Comparison between the two images within the NW-SE vector shows that result from the sliced-filtered image unveils more lineaments and fracture traces.

### 3.2. Discussion

The interpretability of both Landsat ETM+ band 8 and panchromatic aerial photograph in lineament and fracture trace extractions is governed by the way in which shade is expressed in the images. This is quite reasonable since interpretation of lineaments and fracture traces in Gunungsewu Karst is much dependent upon morphological expression of aligned karst hills cut by aligned dry valleys. As previously reported [20], shade is an important image characteristic in expressing relief. In that regard, recording time of the images that have never been discussed in previous works [1, 4, 5, 9, 13, 14, 17, 29, 32] with respect to the shadow resulting from the sun illumination angle is the key factor in the different interpretability of the images for lineament and fracture trace extractions. This reason is attributed to the lack of lineaments and fracture traces in the NE-SW vector resulting from the Landsat ETM+ Band 8 used in this research. The Landsat ETM+ band 8 was recorded in June where sun illumination was parallel to the aligned karst hills in the NE-SW direction. As a result, less shades are depicted in the Landsat ETM+ band 8. Whereas, the aerial photograph used was taken in September when sun illumination made angles to general lineament and fracture trace orientations of the studied area (Figure 6).



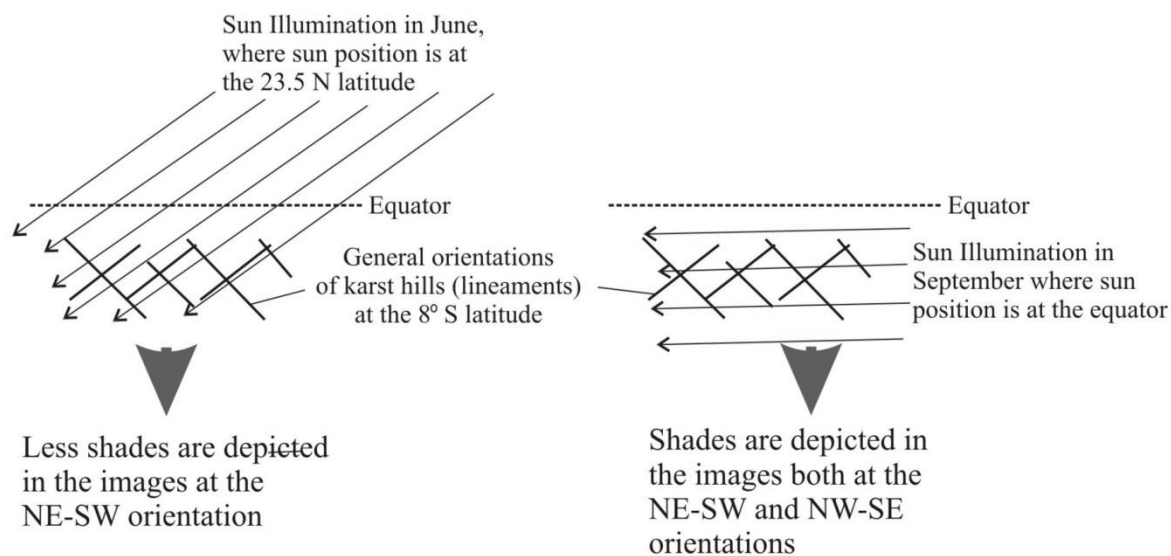


**Figure 6.** Illustration of sun illumination angles with respect to the shade expressed in the images

Undoubtedly, lineaments and fracture traces are better depicted in panchromatic aerial photographs compared to original Landsat ETM+ panchromatic band scenes, as shown by student results. Better resolution of aerial photographs results in detail morphological features including aligned karst hills and aligned dry valleys. This finding is in agreement with Gunawan [6], Kamel & Elsirafe [12], and Kresic [13]. However, Landsat ETM+ panchromatic band can be applied very favorably in lineament fracture trace extraction after being subjected to filtering as shown by the first author interpretation results. Filtering accompanied black and white presentation is found to be a powerful enhancement technique in lineament and fracture trace extractions. Directional filtering enhancing lineaments and fracture traces in this research echoes the results of Suzen & Toprak [29]. Slicing the filtered image to black and white presentation has made the identification of lineaments much easier compared to that from a stretched image as well as to that from aerial photographs. This result confirms the previous work by Haryono & Day [7], and Kresic [13], suggesting successful lineament enhancement of karst terrain from sliced images.

Fragmented lineaments as suggested by Suzen & Toprak [29], due to filtering are not always the case in the present paper. As long as the imposed filter direction is in line with the dominant lineament azimuth, fragmented lineaments are not likely to occur. Morphological expression of lineaments and fracture traces by shades of aligned karst hills in the study area is presumably being the other explanation of the unfragmented lineaments. However, the present research has shown that fragmented lineaments come into sight when the band 8 is convolved by Sobel kernel with NE-SW, EW and NS principal direction. Though a quantitative comparison is not carried out in this paper, the fragmented lineaments seem to be encountered when the direction of the domain spatial filter is not parallel to the dominant lineament azimuth.

Related to vector distribution analysis, care must be taken when deciding between length and frequency used in the analysis. Results of this paper demonstrate that presentation by length is more reliable than by frequency as can be seen from the dominant vector direction. Since filtering will modify the lineaments and fracture traces dimension, length-based analysis will be more reliable, especially when directional filter application causes lineaments fragmentation as it was encountered by Suzen and Toprak [29]. Let alone when the fragmentation does not arise in all direction of spatial domain filters. If this is the case, analysis based on frequency will lead to misinterpretation over the nature of the lineaments and fracture traces.

Frequency distribution of lineaments and fracture traces derived from aerial photograph confirms previous results [4, 7] suggesting dominant vectors of lineaments and fracture trace in the NW-SE and NE-SW directions. These lineaments and fracture traces are associated with joint systems, the so

called Meratus System. These two joint sets are shear fracture resulted from north-south compression associated with tectonic plate convergence of the Hindian-Australian plate and the Eurasian Plate [3, 23, 25, 28, 32]. They are said to be the reactivation of Oligo-Miocene deformation involving the underlying rocks. Faults are likely to occur in the area, however, their field evidence is difficult to be examined [22, 25]. These major structures are represented by dry valley systems of the area [4, 22].

#### 4. Conclusions

The interpretability of both Landsat ETM+ band 8 and panchromatic aerial photograph in lineament and fracture trace extractions is governed by the way in which shade is expressed in the images. In that regard, recording time of the images with respect to the sun illumination angle is the key factor in the interpretability of the images for lineament and fracture trace extractions in structurally controlled conical karst terrain. Lineaments and fracture traces are better depicted in panchromatic aerial photograph compared to original Landsat ETM+ panchromatic band. However, Landsat ETM+ panchromatic band can be very favorable in lineament fracture trace extraction after being digitally enhanced. Filtering accompanied black and white presentation is found to be a powerful enhancement technique in lineament and fracture trace extractions. Presentation by length is more reliable than by frequency in the dominant lineaments and fracture trace direction analyses of conical karst terrain.

#### Acknowledgments

Thanks are due to the Higher Education Directorate of the Indonesian Government, who provided funding through Hibah Bersaing Scheme. We acknowledge the constructive comments on earlier drafts Dr. Paul M. van Dijk.

#### References

- [1] Arellano-Baeza AA, Zverev AT, Malinnikov VA 2006 Study of changes in the lineament structure caused by earthquakes in South America by applying the lineament analysis to the Aster (Terra) satellite data *Advances in Space Research* **37** 690–697
- [2] Bakose GYB 1994 Stereo photo interpretation of karst terrain in the Al Hatra area of Iraq *ITC Journal* **2** 139-144
- [3] Balazs D 1968 Karst regions in Indonesia Karszt Barlangkutatas Volume V
- [4] Brahmantyo B, Puradimaja D J, Bando SSIA 1998 Interpretasi kelurusan dari citra SPOT dan hubungannya dengan pola pengaliran bawah tanah pada perbukitan Karst Gunungsewu Jawa Tengah bagian selatan *Buletin Geologi* **28** (1) 37-49
- [5] Galanos I, Rokos D 2006 A statistical approach in investigating the hydro geological significance of remotely sensed lineaments in the crystalline mountainous terrain of the island of Naxos, Greece *Hydrogeology Journal* **14** 1569–1581
- [6] Gunawan T 1997 The contribution of aerial photographs in evaluation of Bribin Catchment area, GunungKidul, Yogyakarta, Indonesia. *The Indonesian Journal of Geography* **29** 159-176
- [7] Haryono E, Day M 2004 Landform Differentiation within the Gunungkidul Kegelkarst, Java-Indonesia *Journal of Cave and Karst Studies* **66** (2) 62-68
- [8] Haryono E 2000 Some properties of epikarst drainage system in Gunung Kidul Regency Yogyakarta Special Province Indonesia *The Indonesian Journal of Geography* **32**(79-80) 75-86
- [9] Haryono E, Nurcahyo AD, Gunawan T, Purwanto TH 2005 Underground river network modeling from lineaments and fracture traces by means of remote sensing and GIS *Proc of International Conference on Water Resources and Environmental Problems in Karst Belgrade and Kotor*
- [10] Hung LQ, Dinh NQ, Batelaan O, Tam VT, Lagrou D 2002 Remote sensing and GIS-based analysis of cave development in the Suoimuoi Catchment (Son La - NW Vietnam) *Journal of Cave and Karst Studies* **64**(1), 23-33
- [11] Hutington JF, Raiche, AP 1978 Multi-attribute method for comparing geological lineament

- interpretations *Remote Sensing of Environment* **7**(2) 145-161
- [12] Kamel AF, Elsirafe AM 1994 Delineation and analysis of the surface and subsurface structural lineament patterns in the North Lake Nasser area and its surroundings, Aawan, upper Egypt *International Journal of Remote Sensing* **15** (7) 1471-1493
- [13] Kresic N 1995 Remote sensing of tectonic fabric controlling groundwater flow in Dinaric Karst *Remote Sensing of Environment* **53** 85-89
- [14] Leech DP, Treloar PJ, Lucas NS, Grocott J 2003 Landsat TM analysis of fracture patterns a case study from the Coastal Cordillera of northern Chile *International Journal of Remote Sensing* **24** (19) 3709-3726
- [15] Nyborg M, Berglund J, Triumf CA 2007 Detection of lineaments using airborne laser scanning technology Laxemar-Simpevarp Sweden *Hydrogeology Journal* **15** 29–32
- [16] O’Leary DW, Friedman JD, Pohn HA 1976 Lineament, linear lineation some proposed new standards for old terms. *Geological Society of America Bulletin* **87** 1463–1469
- [17] Parcharidis I, Psomiadis E, Stamtis G 1998 Using Landsat TM images to study the karstic phenomenon *ITC Journal* **2** 118-123
- [18] Parizek RR 1976 On the nature and significance of fracture traces and lineaments in carbonate and other terranes *Proceeding Karst Hydrology and Water Resources Volume I Dubrovnic*
- [19] Qari MHT 2010 Lineament extraction from multi-resolution satellite imagery: a pilot study on WadiBani Malik, Jeddah, Kingdom of Saudi Arabia, *Arabian Journal of Geoscience* 2010 DOI 10.1007/s12517-009-0116-3
- [20] Raghavan V, Wadatsumi K, Masumoto S 1993 Automatic extraction of lineament information from satellite images using digital elevation data *Earth and Environmental Science* **2**(2) 148-155
- [21] Rahardjo W, Sukandarrumidi, Rosidi HMD 1995 Geological Map of The Yogyakarta Sheet Java Geological Research and Development Centre: Bandung
- [22] Samodra H 1997 Geological Map Surakarta Quadrangle Geological Directorate Bandung
- [23] Samodra H 2006 Pembentukan lembah kering purba kawasan karst Contoh kasus Gunungsewu In Maryanto I Noerdjito M Ubaidillah R Eds Managemen Bioregional Masalah dan Pemecahannya Dilengkapi Kasus Jabotabek Puslit-Biologi LIPI Bogor
- [24] Solomon S, Quiel F 2006 Groundwater study using remote sensing and geographic information systems (GIS) in the central highlands of Eritrea *Hydrogeology Journal* **14** 729–741
- [25] Suroño BT, Sudarno I, Wiryosujono S 1992 Geology of the Surakarta-Giritontro Quadrangles Java Geological Research and Development Centre. Bandung
- [26] Šušteršič F 2002 Collapse dolines and deflector faults as indicators of karst flow corridors. *International Journal of Speleology* **31**(1/4) 115-127
- [27] Šušteršič F 2006 Relationships between deflector faults collapse doline sand collector channel formation *International Journal of Speleology* **35**(1) 1-12
- [28] Sutoyo 1994 Sikuen stratigrafi karbonat Gunungsewu *Proceedings Pertemuan Ilmiah Tahunan IAGI Ke 23 Jakarta*
- [29] Suzen ML, Toprak V 1997 Filtering of satellite images in geological lineament analyses an application to a fault zone in central Turkey *International Journal of Remote Sensing* **19** (6) 1101-1114
- [30] Tam VT, De Smedt F, Batelaan O, Dassargues A 2004 Study on the relationship between lineaments and borehole specific capacity in a fractured and karstified limestone area in Vietnam *Hydrogeology Journal* **12** 662–673
- [31] Tripathi NK, Gokhale KVG 2000 Directional morphological image transforms for lineament extraction from remotely sensed images *International Journal of Remote Sensing* **21** (17) 3281-3292
- [32] Van Bemmelen RW 1970 The Geology of Indonesia Volume 1A General Geology Martinus Nijhoff The Hague
- [33] Zakir FA, Qary MHT, Mostafa ME 1999 A new optimizing techniques for preparing lineament density maps *International Journal of Remote Sensing* **20** (6) 1073-1085